



Research article

Design of a sensor to estimate suspended sediment transport *in situ* using the measurements of water velocity, suspended sediment concentration and depth

T. Matos^{a,*}, M.S. Martins^b, Renato Henriques^c, L.M. Goncalves^{a,d}

^a CMEMS, University of Minho, Campus de Azurém, Guimarães, Portugal

^b INESC TEC, Faculdade de Engenharia da Universidade do Porto, Porto, Portugal

^c Institute of Earth Sciences, University of Minho, Campus de Gualtar, Braga, Portugal

^d LABBELS –Associate Laboratory, Braga/Guimaraes, Portugal



ARTICLE INFO

Handling editor: Jason Michael Evans

Index Terms:

Sediment transport
Water velocity
Suspended sediment concentration
Water discharge
Transport rate
Sensor

ABSTRACT

— The sediment transport plays a major role in every aquatic ecosystem. However, the lack of instruments to monitor this process has been an obstacle to understanding its effects. We present the design of a single sensor built to measure water velocity, suspended sediment concentration and depth *in situ*, and how to associate the three variables to estimate and analyse sediment transport. During the laboratory calibrations, the developed instrument presented a resolution from 0.001 g/L to 0.1 g/L in the 0–12 g/L range for the measurement of suspended sediment concentration and 0.05 m/s resolution for 0–0.5 m/s range and 0.001 m/s resolution for 0.5–1 m/s range for the measurement of water velocity. The device was deployed for 6 days in an estuarine area with high sediment dynamics to evaluate its performance. During the field experiment, the sensor successfully measured the tidal cycles and consequent change of flow directions, and the suspended sediment concentration in the area. These measurements allowed to estimate water discharge and sediment transport rates during the different phases of tides, and the daily total volume of water and total amount of sediment passing through the estuary.

1. Introduction

Sediment transport, or sediment load, is the movement of organic and inorganic particles in water. Sediment transport is directly influenced by water discharge, which allows for suspension and resuspension of particles. When the flow rate is strong enough, some smaller and lighter particles in the streambed can be lifted into the water column and become suspended. These particles either move downstream in suspension or are pushed along the bottom of the waterway. In general, a higher flow rate results in more sediment being transported. When there is not enough water flow to move the suspended material, it will settle at the bottom of the stream (Chien and Wan, 1999). It is important to notice that suspended load and suspended sediment are not the same, even if it is often overlap. Suspended sediment is any particles found in the water column, whether the water is flowing or not. Suspended load is the amount of sediment carried downstream within the water column by the water flow. Suspended load requires moving water, as the water flow

creates small upward currents (turbulence) that keep the particles above the streambed (Furukawa et al., 1997).

Water flow, also referred to as water discharge, is the single most important element of sediment transport. The flow of the water body is responsible for picking up, moving and depositing sediments in a watercourse (Knighton, 1999). Without flow, sediment transport would not exist and the particles would remain suspended or settle out without downstream movement. Most changes in water flow are due to weather events such as rainfall. Precipitation causes water levels to initially rise, and then return to the previous base flow level over the course of hours or days. Rainfall, whether slight or heavy, can affect water flow and sediment transport. The extent to which a weather event will influence sediment transport is dependent on the amount of sediment available. Heavy rainfall over an area of loose soil and minimal vegetation will create runoff, carrying loose particles into the waterway (Guzman et al., 2013). Likewise, flooding will also pick up sediment from the area. Even though sediment is important all along the watershed, it has gathered

* Corresponding author.

E-mail address: matos.tiagoandre@cmems.uminho.pt (T. Matos).

<https://doi.org/10.1016/j.jenvman.2024.121660>

Received 29 December 2023; Received in revised form 6 June 2024; Accepted 29 June 2024

Available online 3 July 2024

0301-4797/© 2024 The Authors. Published by Elsevier Ltd. This is an open access article under the CC BY license (<http://creativecommons.org/licenses/by/4.0/>).

significant attention in the coastal areas due to the emerging problems related to climate change, sea level rise and coastal erosion. In these areas, other agents of sediment transport must be considered, such as wind activity (that produces waves and surface currents), tides, storm surges and near-shore currents (Lou and Ridd, 1997).

In the last decades, several computational models have been presented to predict sediment transport (Schmeeckle, 2014; Kiat et al., 2008; Duan and Nanda, 2006; Yanto and Dimiyati, 2023; Zheng et al., 2023). These models are accurate to a certain point (Papanicolaou et al., 2008). The high complexity of real scenarios and the limitations of the models make it a very difficult task to produce results with detail. The complexity of sediment transport rates is affected by innumerable variables such as the bed geometry, particle size statistics (e.g. average size, standard deviation, kurtosis, asymmetry), shape and concentration, and the multiple forces acting upon the sediment as relative inertia, turbulent eddies or velocity fluctuations in speed and direction (Southard, 2006). Most flow rate and sediment transport rate equations attempt to simplify the scenario by ignoring the effects of channel width, shape and curvature of a channel, sediment cohesion and non-uniform flows. The use of monitoring data is usually referenced as one of the most important methods to improve the accuracy of said models. These data, provided by sensors deployed *in situ*, can be used both as input for the models and to validate their results. However, the current state of the art of monitoring instruments for sediment transport has limitations.

Sediment transport is a combination of suspended sediment concentration and water flow. However, monitoring sensors focus on those variables independently. Turbidity sensors are used for continuous monitoring of sedimentary dynamics in the field (Skarbøvik et al., 2023; Druine et al., 2018; Mitchell et al., 2003; Rymszewicz et al., 2017). These instruments can use optical or acoustic technology and provide discrete measurements of turbidity (usually in standard units as NTU) or concentration of suspended particle matter (in g/L). The measuring of water discharge is also needed for a full comprehension of sediment transport. For this case, acoustic instruments based on time-of-flight or doppler effect can be used (Wullenweber et al., 2022; Liu et al., 2022). Doppler technology uses the frequency shift of backscattered acoustic echoes to calculate water velocity. The received acoustic power of these echoes can also estimate suspended sediment concentration, following the same principle as turbidity backscatter acoustic sensors (Sahin et al., 2020; Munandar Manik; Firdaus, 2021; Chalov et al., 2022). Since instruments based on this technology can measure both water velocity and sediment concentration, they are the closest to a single sensor that can measure sediment transport (Nord et al., 2014; Kostaschuk et al., 2005). Yet, Doppler technology to measure sediment concentration lacks accuracy, mostly when compared to its optical peers. In addition, the available commercial instruments, both turbidity sensors and current meters, present high prices that can range from some thousand to dozens of thousands of euros. This poses a limitation for large-scale deployments necessary to understand environmental dynamics and provide data for computational models.

We presented before fully automatic instruments to measure turbidity (T. Matos et al., 2019) and sediment deposition and erosion of the streambed (T. Matos et al., 2022) for environmental monitoring. These instruments have been developed considering the need for reduced costs and high energy efficiency. In a continuation of this work, we present in this manuscript the design of a new sensor focused on the measurement and evaluation of sediment transport for continuous monitoring *in situ*. Two outcomes are expected from this work: the design and validation of a sensor that aims to evaluate sediment transport by the measurement of water velocity, suspended sediment concentration and depth and to raise awareness for the potential of using this kind of device to understand sediment dynamics of coastal areas.

2. Material and methods

2.1. Sensor design

Following the development of low-power and low-cost monitoring instruments presented before, a new sensor was built to measure the concentration of suspended sediment and water velocity. Additionally, and since the sensor is intended to be deployed in an estuarine area subject to tides, a TE Connectivity MS5837-30BA integrated circuit was integrated into the instrument to measure water temperature and pressure (used to calculate water depth).

The suspended sediment concentration is measured using direct light detection in the infrared wavelength. This method offers a broader detection range compared to common techniques such as backscattering or nephelometry, which is crucial for understanding sedimentary dynamics in estuaries. Additionally, using infrared light reduces interference from solar radiation due to the higher absorption of this wavelength by water. This optical technology was tested and validated before in instruments developed to measure turbidity and suspended particulate matter (T. Matos et al., 2019, 2020, 2022). The new sensor uses an optical channel with a 45 mm light path that comprises a VSLY5940 light emitting diode (LED) as the light source (940 nm wavelength, $\pm 3^\circ$ angle of half intensity and 600 mW/sr radiant intensity at 100 mA), and a BPV11F phototransistor as the light detector (940 nm wavelength, $\pm 15^\circ$ angle of half sensitivity and 1 nA dark current). The principle of operation to measure suspended sediment concentration relies on the absorbance and scattering of the emitted light, which decreases the luminosity sensed by the receiver (top-left image of Fig. 1). Thus, clean water produces the highest voltage output that decreases with the existence of suspended matter.

A cantilever using four strain gauges TENMEX TF3/120-K (120 Ω nominal resistance, $\pm 0.5\%$ tolerance and $5 \times 7.5 \times 0.06$ mm dimension) in a full-Wheatstone bridge was designed to measure the water velocity. The strain gauges are mounted on the bridge in a typical pair of compression/decompression configurations to enhance temperature compensation, increase sensitivity, and measure fluid velocity in two directions. Two of the strain gauges were glued using cyanoacrylate on the top of a $20 \times 80 \times 0.2$ mm acetate strip and the other two on its bottom back-to-back to the front strain gauges. The acetate strip and strain gauges are embedded in room-temperature-vulcanizing (RVT) elastomer silicone (HB Flex 901 Silicone RTV-2, HBQuimica) to meet the water-tight needs. Supplementary Material 1 presents the fabrication of the cantilever. The principle of operation to measure water velocity relies on the bending of the cantilever when subject to the drag force of the stream flow. This bending causes the mechanical extension and compression of the strain gauges and generates an electric output in the Wheatstone bridge (bottom-left image of Fig. 1). The presented design of the cantilever allows the sensor to measure fluid velocity in 1-axis and both directions.

A printed circuit board (PCB) was designed with the electronic instrumentation for the transduction mechanisms. An AD8227 instrument amplifier amplifies the electrical output of the Wheatstone bridge that is read by the analogue-to-digital converter (ADC) of a low-power STM32L412K8T6 microprocessor. The same microprocessor controls the LED turning it on and off with a DMG6968U-7 MOSFET, reads the electrical output of the photodetector and hosts the MS5837-30BA component that measures water temperature and pressure. The electronics are powered by a battery or any other source of energy that supplies a TPS62840DLR voltage converter. The sensor uses an LTC1480 RS-485 interface module for serial communications, allowing the instrument to be connected to a computer or data logger.

The complete electronic schematic can be consulted in Supplementary Material 2 and the PCB in Supplementary Material 3, so that the sensor can be replicated by the scientific community. The presented electronic design results in a power consumption of 250 mW taking measurements (≈ 8 ms) and 6 μ W in sleep mode. The structural housing

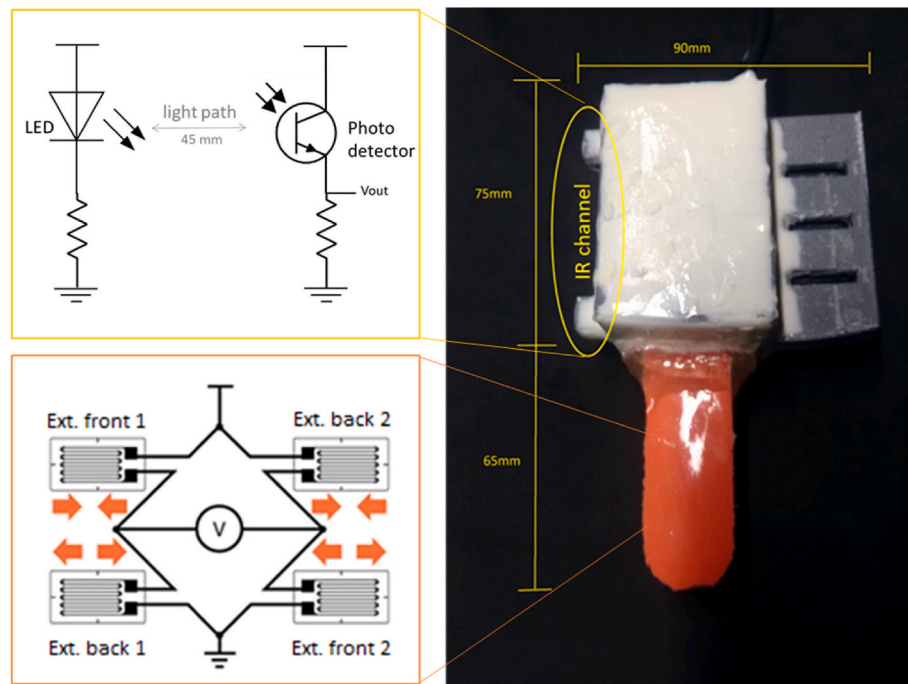


Fig. 1. Illustrations of the transduction mechanisms of the instrument. The top-left image shows the arrangement of the strain gauges in a full-Wheatstone bridge to measure the water velocity. The top-right image shows the simplified electronic circuit of the LED and photodetector used for the optical channel to measure suspended sediment concentration. The bottom-left image shows a photograph of the sensor.

was 3D-printed in acrylonitrile butadiene styrene (ABS) material to assemble the cantilever, optical channel, temperature and pressure sensors and comprise the PCB. The 3D drawing is presented in [Supplementary Material 4](#). The inside of the housing was filled with polyurethane material (HB R 16/25—HBQUIMICA) to protect the electronics from the water. The sensor is plugged by an electric cable that shares power and serial communications. The instrument had a total cost of 70 € in raw materials. The right image of right image of [Fig. 1](#) presents the final appearance of the instrument.

2.2. In-lab calibrations

A set of laboratory experiments were conducted to calibrate the sensor to be able to estimate sediment transport *in situ*. The water depth is an indirect measurement of the pressure sensor that does not require calibration. The other two variables that the sensor measures are suspended sediment concentration (or turbidity) and water velocity. Setups of laboratory experiments were designed to correlate both the electrical output of the photodetector to different suspended sediment concentration and the electrical output of the Wheatstone bridge to different fluid velocity in two directions. An additional test of water temperature was conducted to mitigate the susceptibility of the strain gauges and remaining electronics to temperature variations.

2.2.1. Suspended sediment concentration

The optical channel output of the sensor can be calibrated in turbidity units using standard formazin solutions or in suspended sediment concentration. Since the objective of the developed sensor is to measure sediment transport, the calibration with formazin was ignored for this work. Both calibrations using formazin and suspended sediment sand were presented before for a suspended particulate matter sensor (T. Matos et al., 2019). For the case of suspended sediment, the calibration conducted before showed that different sizes of sediment produce different output results. Since sediment transport is highly influenced by wash load, the sediment calibration of the developed sensor was conducted using small particle sizes.

Seashore from the place where the sensor was intended to be installed (estuary of Cávado River, Portugal) was collected and sieved using a 125 μm American Society for Testing Materials (ASTM) sieve. The sensor was submerged in a container with distilled water and the prepared seashore sand was gradually added to the sample. Before every measurement, a mechanical mixer was used to homogenize the sample and resuspend any settled sediment. It was observed that with the used particle size, the sediment remained in suspension on the water and took more than 30 s to settle after the sample was agitated. Twenty measurements with a sampling period of 0.5 s were taken for suspended sediment concentration of 0, 0.1, 0.23, 0.35, 0.46, 0.59, 0.7, 0.88, 1.07, 1.22, 1.37, 1.66, 1.85, 2.33, 3.04, 4.05, 5.09, 6.62, 9.14 and 11.68 g/L (consult [Supplementary Material 5](#) for samples comparison).

[Fig. 2](#) shows a boxplot graph with the maximum, minimum, mean and outliers (red crosses) of the calibration measurements. The results show the expected behaviour of a transmitted light detection technique. The sensor recorded maximum output values for the distilled water sample (0 g/L) that decreases with the increment of sediment in the water that scatters and absorbs the transmitted light. The sensitivity decreases from 656 to 9.3 mV(g/L), in the range 0–12 g/L. Considering the output voltage and the 12-bit ADC, the resolution of the sensor decreases from 0.001 g/L to 0.1 g/L in the same range. The higher resolution in the range of 0–4 g/L provides the necessary limit of detection for *in situ* monitoring. The curve fitting of the correlation between the sensor output (mV) and the sediment concentration (g/L) was computed and embedded in the firmware of the sensor for the field experiment.

The combination of low depth, clean waters and intense sunlight can interfere with the measurements and produce errors in the estimation of the suspended sediment concentration. The use of infrared light, which has a higher light absorption on water compared to smaller wavelengths, is used to reduce this effect. Nevertheless, a compensation for the effect of external light was implemented as demonstrated in previous work with turbidity sensors (T. Matos et al., 2019).

2.2.2. Water velocity

The other variable measured by the sensor is water velocity. A testing

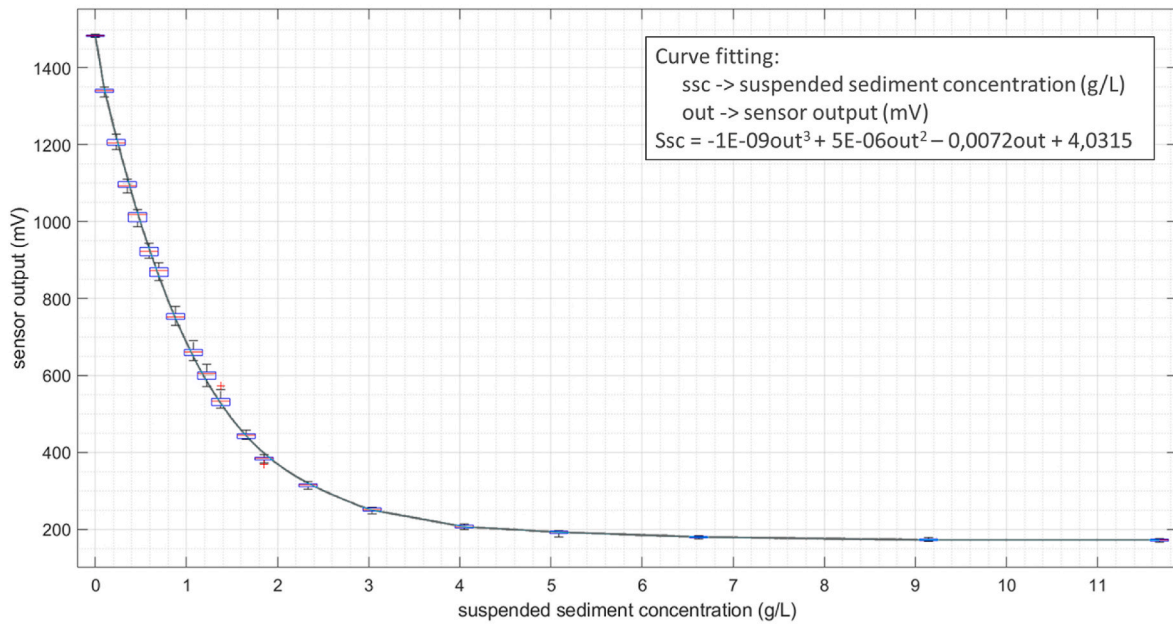


Fig. 2. Calibration results for suspended sediment concentration. The boxplot graph shows the records of the sensor for different concentration of seashore sand. Outliers are shown in red crosses. The curve fitting was computed to be embedded in the software of the sensor for the *in situ* experiments.

setup was prepared to calibrate the sensor to different flow magnitudes that consisted of a water circuit composed of a water pump, a closed chamber with the sensor and water channels/connections (illustration scheme of the test setup presented in Supplementary Material 6). Two different water pumps were used to generate 18 flow intensities: Jebao DC-650 pump (8 intensity levels) and Jebao DC-4000 (10 intensity levels). For each one of the 18 flow intensities, the water circuit was opened to measure the discharge and the corresponding water velocity was calculated using Equation (1) and using the cross-section area of the sensor chamber. For each flow intensity, the sensor recorded 20 measurements with a sampling period of 1 s. After the experiment, the inlet and outlet of the sensor chamber were inverted, and the test was conducted again to measure the water velocity in the contrary direction.

$$discharge [m^3 / s] = area [m^2] * velocity [m / s] \tag{1}$$

Fig. 3 shows the results of the calibration experiment with both water pumps in a boxplot graph (median, minimum, maximum and outliers). The Jebao DC-650 pump (red boxplots) produced flows from 0.094 to 0.752 m/s in the downstream and upstream directions (red box plots in Fig. 3). The Jebao DC-4000 pump (blue boxplots) produced higher flows in both directions (blue box plots in Fig. 3). The results with the different pumps are coherent with each other. The records for 0 m/s and from 0.5 m/s to 0.752 m/s (common ranges for both pumps) are similar. The graph shows that the variance of the measurements increased for higher flow rates and mostly for the Jebao DC-4000 pump. This behaviour happens because the turbulence inside the chamber of the sensor

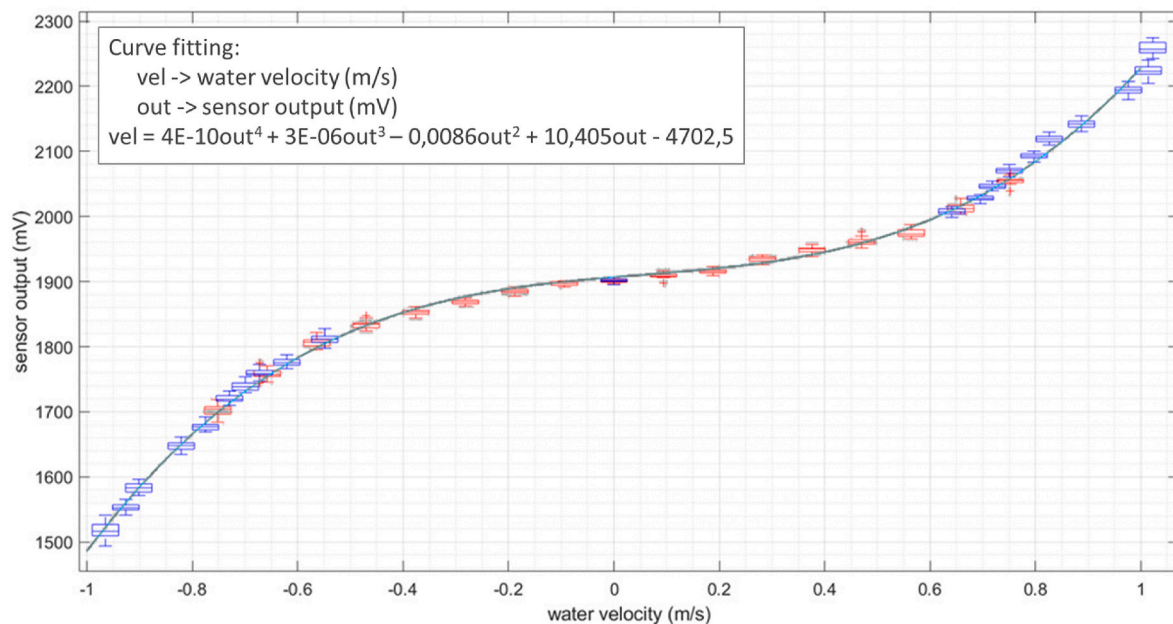


Fig. 3. Calibration results for water velocity. The boxplot graph shows the records using the Jebao DC-650 pump in red and the records using the Jebao DC-4000 in blue. Outliers are shown in red crosses. The curve fitting was computed to be embedded in the software of the sensor for the *in situ* experiments.

increases with higher flows. The sensor presented a sensitivity of ≈ 135.28 mV/(m/s) and 0.05 m/s resolution in the range $|\text{velocity}| < 0.5$ m/s, and ≈ 578.17 mV/(m/s) and 0.001 m/s resolution in the range $0.5 < |\text{velocity}| < 1$ m/s. The curve fitting of the data was computed using a 4-order polynomial curve (cyan line in the graph of Fig. 3) to correlate the sensor output (mV) to values of water velocity (m/s). The curve was embedded in the firmware of the sensor for the field experiment.

2.2.3. Temperature calibration

The major factor that can produce errors in the velocity measurements is the susceptibility of the strain gauges of the cantilever and electronics to temperature. Even though the full-Wheatstone bridge is used to reduce this error, an experiment was conducted to analyse the response of the sensor to different water temperature.

The sensor was placed in a container with still water at 25 °C and ice. The instrument took records with a sample period of 5 s till the water temperature reached 10 °C (the temperature was measured by the MS5837-30BA sensor). The top-left graph of Fig. 4 shows the measurements recorded during the experiment. Since there is no flow in the container, for a good operation the output of the sensor should be constant. However, the results show that the temperature affects the output and a calibration is needed to correct the output as a function of the water temperature.

The first step is to divide the measurements by the corresponding output value for 0 m/s (there was no water flow in the container during the experiment). According to the calibration for water velocity presented in the previous section, the output value that corresponds to 0 m/s is 1901 mV (the water velocity calibration was performed with water at 15 °C). The top-right graph of Fig. 4 shows the relative coefficient of this division. Note that the coefficient value of 1 corresponds to the water temperature of 15 °C, as supposed. The coefficient function was fitted in a 3-order polynomial curve that is used to rectify the sensor output as a function of the water temperature according to the following equation:

$$\text{output}_{\text{rectified}} = \frac{\text{output}_{\text{measured}}}{f_{\text{coefficient}}(\text{temperature})} \quad (2)$$

The bottom graph of Fig. 4 shows the temperature calibration applied to the experimental data. The results show that the algorithm developed reduces the susceptibility of the sensor to water temperature, presenting a calibrated output with minimal variation.

2.3. Field experiment setup

After the laboratory calibrations, the sensor was installed in the estuary of Cávado (41°31'56.84"N, 8°47'4.16"W; Esposende, Portugal) to validate its potential to estimate sediment transport. The estuary of Cávado is characterized by shallow waters and high sedimentary dynamics that have been causing several problems in the proper navigation of the estuary and are a major issue for the effective protection of the urbanized coastal line during storms. This coastal region has been suffering changes in its geomorphology during the last decades (Loureiro et al., 2005). The uncertainty about the sediment dynamics in this location makes it attractive for the use of technology that can gather data for a better understanding of the area. For this reason, we have been using the estuary to test and validate sensors to measure different water parameters (T. Matos et al., 2022).

The developed instrument was installed *in situ* from the 26th of May to the 1st of June of 2023. The device was fixed to a stainless steel structure buried in the estuary bed using an Archimedes screw. The instrument was placed 90 cm above the bed and with the cantilever and optical channel perpendicular to the streambed. An illustration of the installation setup is presented in Supplementary Material 7. The sensor was connected by an electric cable that shares power and RS485 communications to an external data logger placed outside the water. The data logger consisted of an own-developed microcontroller based on an STM32 processor with a real-time clock (to keep time and date) and

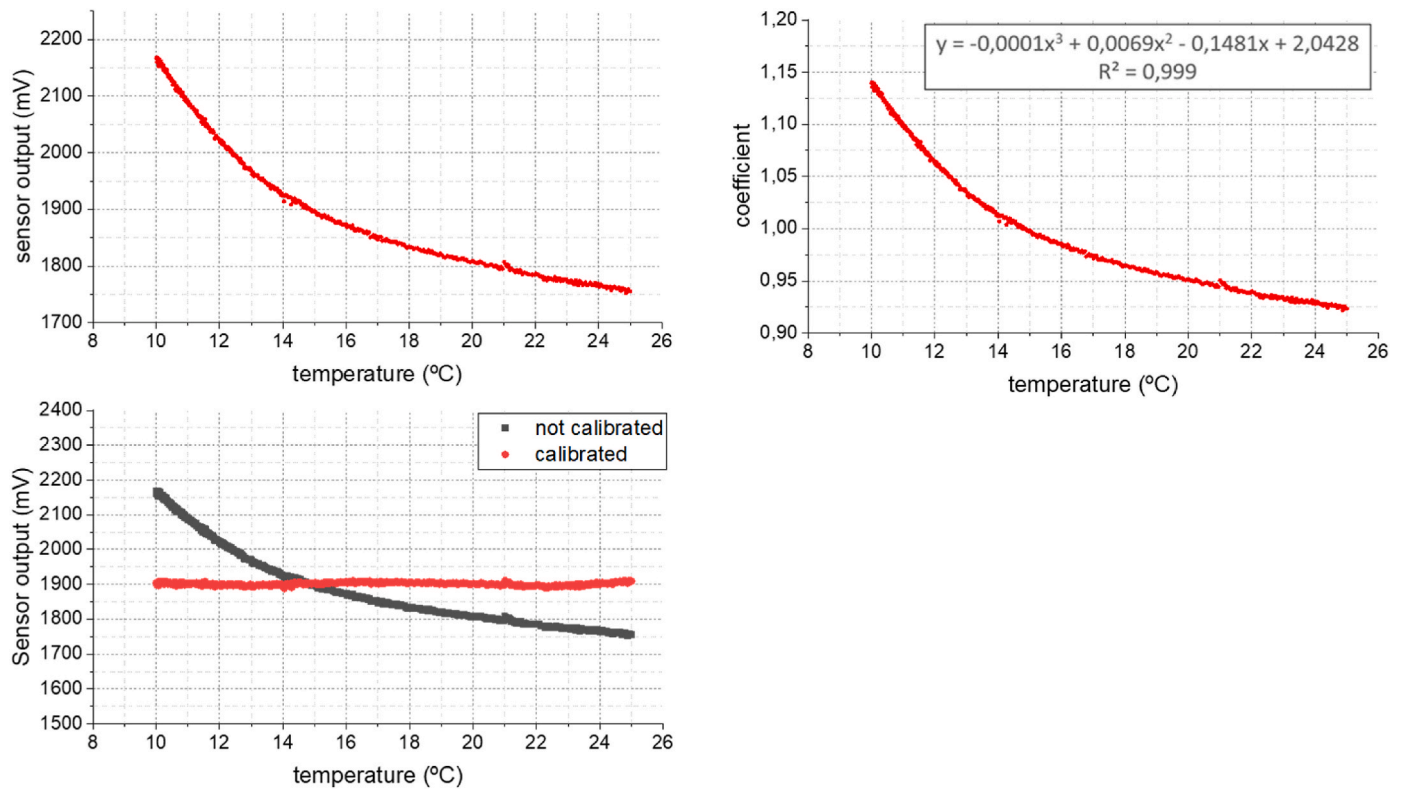


Fig. 4. Calibration results for water temperature. The top-left graph shows the measurements of the sensor during the experiment with different water temperature. The top-right graph shows the coefficients curve using the sensor output corresponding to 0 m/s as reference (1901 mV). The bottom graph shows the final result comparing the calibrated and not calibrated curves.

microSD card module (to store the data). The whole system was powered by a 3.3V 2000 mAh LiPo battery and has 1 year of autonomy taking measurements every 1 min.

The sensor was set to take measurements every 5 min of water velocity, suspended sediment concentration, pressure and water temperature. The sensor was set to take 20 measurements of each variable and calculate the average value. To estimate the values of water velocity, the electrical output of the cantilever of the sensor is first corrected using the temperature calibration algorithm presented before and then correlated to values of velocity using the mathematical expression computed during the in-lab calibration with the water pump circuits. The data of depth is calculated using the pressure values from the pressure sensor. The values of suspended sediment concentration are calculated using the electrical output of the optical channel with the mathematical expressions computed during the in-lab calibration with seashore sand. The values of suspended sediment concentration are corrected with the external light calibration algorithm if the sunlight produces interference with the data. Sediment transport is then estimated using the values from previous variables, as described hereafter.

2.4. Sediment transport analysis methodology

Sediment transport can be calculated using the measurements of water discharge and suspended sediment concentration. The first step is to calculate the function of water discharge using Equation (1). The values of water velocity are direct measurements of the sensor. The area is related to the cross-section of the river (width and height) where the measurements are taken. Even though the water height is not uniform along the river width, a practical estimation can be done using the depth values measured by the MS5837-30BA. Using the recorded data of water velocity and depth, and a river width of 385 m (river width estimation of the cross section where the sensor was installed, obtained from aerial imagery) a gross approximation of the water discharge can be calculated by the following mathematical expression:

$$\text{water.discharge} [m^3 / s] = \text{river.width} [m] * \text{river.depth} [m] * \text{water.velocity} [m / s] \quad (3)$$

Using constant depth and width implies the approximation of the river cross-section to a rectangular area. Also, the water velocity is assumed to be the same at every point of the cross-section. These assumptions inaccurately represent reality, as the estuary's depth varies across its width and water velocity exhibits complex vertical and horizontal profiles, potentially leading to estimation errors. These implications are examined further in the Discussion section.

Additionally, the total volume of water that flows on the river can be estimated with an approximation of the integration of the water discharge function:

$$\text{total.water.volume}(t) = \sum_{i=0}^{n-1} \text{water.discharge}(t_i) * \Delta t \quad (4)$$

Having the water discharge calculated, the final step is to calculate the sediment transport rate. The transport rate is defined by the amount of sediment flowing along the course of water and can be calculated by Equation (5). Similarly to previous assumptions, for simplification purposes, it is assumed that the suspended sediment concentration remains uniform across every point of the estuary cross-section.

$$\text{transport.rate} [kg / s] = \text{water.discharge} [m^3 / s] * \text{suspended.sediement} [g / L] \quad (5)$$

The total amount of sediment flowing in the estuary can also be estimated with an approximation of the integration of the transport rate function as follows:

$$\text{total.sediment}(t) = \sum_{i=0}^{n-1} \text{transport.rate}(t_i) * \Delta t \quad (6)$$

3. Results

The top-graph of Fig. 5 shows the measurements of water velocity and depth during the first 3 days of the field experiment. The water velocity axis (left y-axis) is presented with positive and negative values. The cantilever of the sensor was positioned to measure positive values for the downstream and negative values for the upstream directions. The data shows that the water velocity intensifies during the peaks of low and high tides. These are the moments when there is maximum water velocity for the downstream and upstream directions, respectively. It is possible to observe the change of the stream direction during the middle of the rising and leaking of tides.

The depth data presents a tidal amplitude of ≈ 1.5 m. This information together with the event of inversion of the flow direction indicates that, during the high tide, the location where the sensor was installed is completely invaded by the ocean. The measurements of the sensor are compliant with the phenomena expected in estuary areas close to the mouth of the river. During the low tide, there is a normal flow of the river in the downstream direction. With the rise of the tide, the water level increases due to the entering of oceanic water in the estuary and the flow velocity decreases. If the location is close enough to the estuary inlet (as is the case of the installation of the sensor), the water stream can invert with the water flowing in the upstream direction.

During the first days of operation, the instrument presented reliable data, without outliers or other erroneous measurements. However, this field experiment was marked by extreme algae blooms phenomena and the estuary became full of macro flora. This event led the cantilever to get stuck in algae and stop delivering reliable measurements. At the end

of the 29th of May, the values of water velocity increased erroneously to a medium value of almost 5 m/s. When the sensor was recovered, it was seen that the cantilever was stuck in algae, forced into the downstream direction, and could not bend properly to measure water velocity (top-right photograph of Fig. 5). [Supplementary Material 8](#) presents the complete data on water velocity during the six days of the experiment.

The bottom-graph of Fig. 5 shows the measurements of suspended sediment concentration, the other variable needed to analyse sediment transport. The test started on the 26th of May with a suspended sediment concentration of ≈ 0.6 g/L that gradually increased during the 28th of May. While this behaviour typically matches the beginning of biofouling attachment on the surface of the optical transducers, the sediment concentration decreased during the 30th of May. A possible explanation is that the 28th to the 30th of May were the days when the algae bloom appeared or intensified, increasing the suspended load in the estuary.

The experiment ended on the 1st of June when the optical channel of the sensor was obstructed with algae. It is possible to observe an abrupt increase in the suspended sediment concentration to 4.5 g/L. This sudden increment in the sediment concentration is a typical behaviour that happens when the measuring channel is partially or totally obstructed. The natural change of suspended sediment in the watersheds is expected to be smoother. When the sensor was recovered, it was confirmed that the instrument was wrapped in algae. After the sensor was recovered

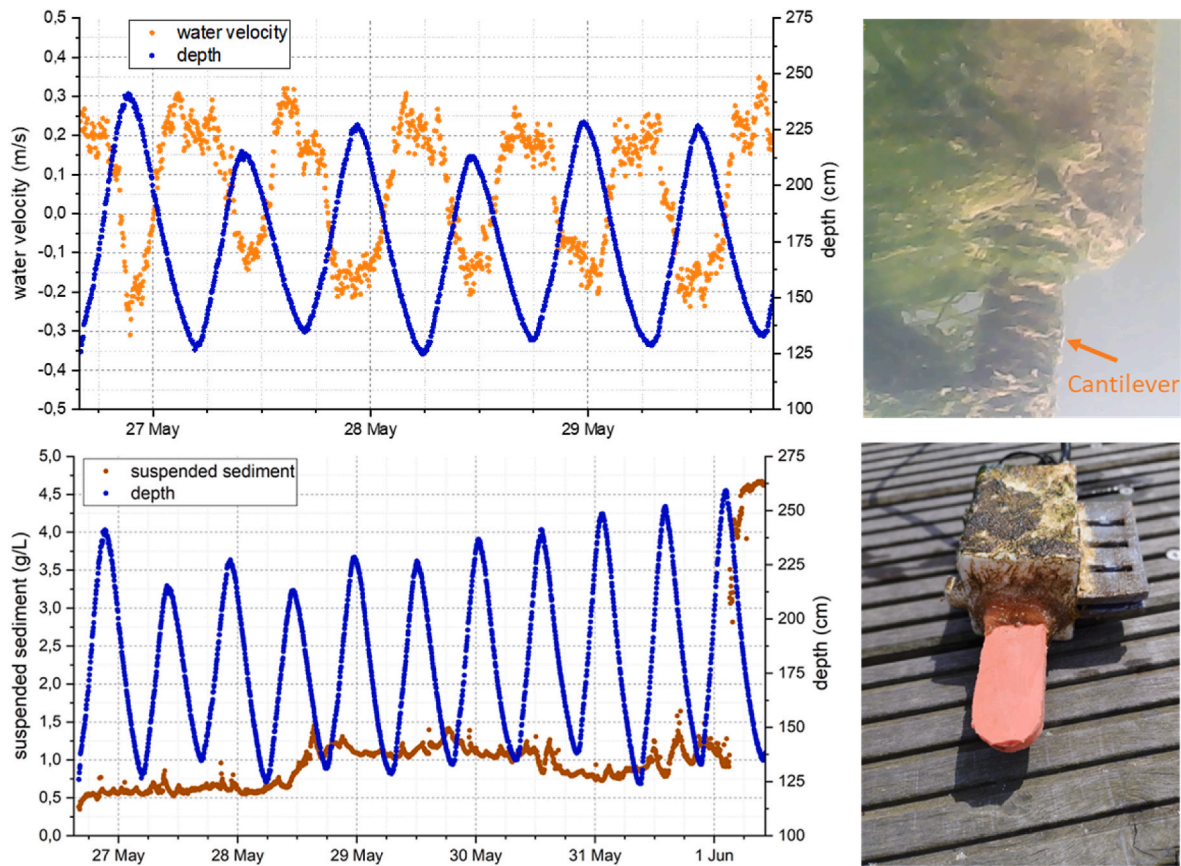


Fig. 5. Monitoring results of the field experiment. The top-graph shows in orange circles the water velocity (left y-axis) and in blue circles the water depth (right y-axis) measured during the first days of deployment. The bottom-graph shows in brown circles the suspended sediment concentration (left y-axis) and in blue circles the water depth (right y-axis). The top-right photograph shows the sensor stuck in algae and the bottom-right photograph shows the instrument after recovery.

and the macrofauna removed, the device did not present visual damages in the cantilever or optical channel. The structure had encrusted biological and geological residues, as the bottom-right photograph of Fig. 5 shows, but the surfaces of the cantilever and optical transducers were clean.

3.1. Sediment transport analysis

The sediment transport can be estimated and analysed using the data of water velocity, suspended sediment concentration and depth measured by the sensor. The data recorded from the 26th to the 29th of May, while the cantilever was producing reliable measurements of water velocity, is used in this sub-section as demonstration.

The estimation of water discharge and total volume of water are presented in the top-graph of Fig. 6 and were calculated using Equations (3) and (4), respectively. Compared with the measurements of water velocity presented in the top-graph of Fig. 5, some details must be noticed. The sensor measured higher water velocity during the low tides ($\approx 0.2\text{--}0.3$ m/s) compared with the high tides ($\approx 0.1\text{--}0.2$ m/s). However, this difference is less evident in the water discharge data. The water discharge considers not only the water velocity but also depth. Thus, the low tides are marked by higher current and lower depth (smaller cross-section area) and the high tides by lower current but higher depth (larger cross-section area). This correlation between water velocity and depth for the different tidal cycles balances the discharge intensity estimated by the sensor. During the low tide (normal flow of the river), the sensor estimated maximum water discharge of $100\text{--}200$ m³/s. These values are in accordance with a monitoring station from Sistema Nacional de Informação de Recursos Hídricos (<https://snirh.apambiente.pt/>), installed 16 km upstream of the deployment location of the

sensor, that has measured water discharge from 30 to 250 m³/s from 1990 to 2017.

Even though the water discharge intensity is similar for the peak of low and high tides, their duration is rather different. The period when the mass of water is flowing upstream (from the ocean to the river) is smaller than when flowing downstream (from the river to the ocean). This event has a direct impact on the total volume of water that infers the average flow direction by the accumulation of water discharge over time. The calculated data of the total volume of water shows that its average value is increasing. This means that, in the installation location of the sensor, the water is flowing predominantly in the downstream direction. Even though this is the normal behaviour of a river (water flowing downstream), it is important to understand that this location is close to the river mouth and is highly influenced by the ocean. The closer the point of collection is from the river mouth, the more influence of the ocean and less influence of the river are expected, decreasing the slope of the total volume of water function.

Considering the two complete days of monitoring (27th and 28th of May), the data presents an accumulative total volume of water flowing from the river to the ocean of $\approx 3\text{M}$ m³/day. The duration of the experiment is small to draw conclusions, but the data available indicates that during the time of the experiment the amount of volume of water per day decreases from day to day. A plausible explanation for this event is that the test was conducted during the transition period from the neap to the spring tide. This means that from day to day the influence of the ocean intensifies, which may cause an increase in the intensity and duration time of the water discharge in the upstream direction.

The bottom-graph of Fig. 6 shows the sediment transport rate, calculated using the data of water discharge and the measurements of suspended sediment concentration according to Equation (5).

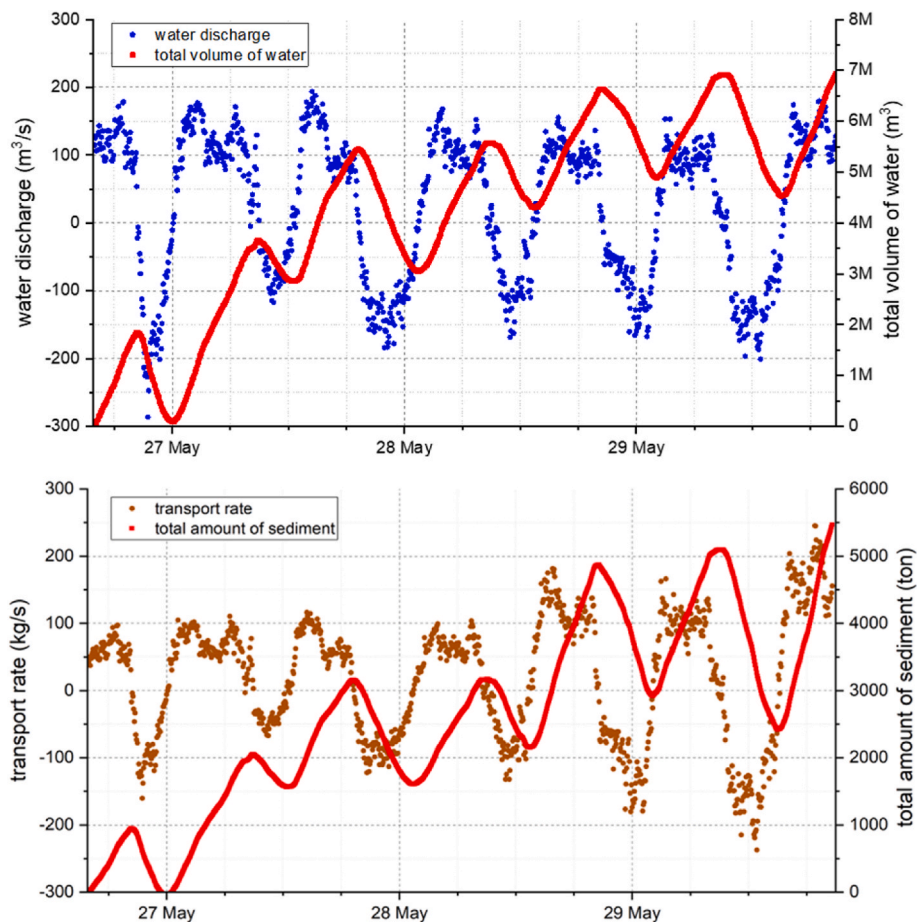


Fig. 6. Estimation of water discharge, total volume of water, sediment transport rate and total amount of sediment. The top-graph shows in blue circles the estimation of water discharge using the measurements of water velocity and depth, and in red squares the total volume of water. The bottom-graph shows in brown circles the estimation of sediment transport rate using the data of water discharge and the measurements of suspended sediment concentration, and in red squares the total amount of sediment.

Additionally, the total amount of suspended sediment was calculated using Equation (6). Since the suspended sediment concentration measured did not present significant variations (bottom-graph of Fig. 5), the resulting signal of the sediment transport rate is shaped by the water discharge data. As before, positive values of transport rate mean that the sediment is flowing in the downstream direction and negative ones in the upstream direction.

The higher transport rates occurred during the peak of the low and high tides derived from the higher discharge intensity registered during these periods. The graph shows maximum transport rates of 50–200 kg/s which are plausible values for small rivers such as the Cávado River. The total amount of sediment indicates that most of the sediment is flowing from the river to the ocean. However, it does not mean that all this sediment has its origin in the course of water upstream the installation of the sensor. Since the location of the experiment was close to the river mouth, most of this sediment is expected to be a continuous suspension and resuspension of the same particles circulating in the estuary. The data shows an accumulative of 2000 tons of sediment per day, flowing from the river to the ocean, during the two complete days of the experiment.

4. Discussion

The developed instrument was validated in the field, providing *in situ* measurements of suspended sediment concentration, water velocity, and depth. These three variables were subsequently used to estimate water discharge, total water volume, suspended sediment transport, and

the total amount of sediment in the estuary. While the operation of the instrument is enhanced by the field experiment, it is important to emphasize that this work delves into technology development and its application. Therefore, the presented field experiment should not be misconstrued as a case study, nor should its estimates of water discharge and sediment transport be considered definitive ground truth measurements. Several considerations must be taken into account regarding the decisions made during this work.

4.1. Calibration considerations

The calibration is a critical aspect in preparing the instrument for *in situ* monitoring and ensuring that the measurements accurately reflect the physical processes in real environment. The measurements of suspended sediment concentration were calibrated using wash load from the field (<125 μm seashore sand) that remained suspended and provided homogeneity in the sample. However, due to water currents and turbulence, this homogeneity does not always occur in the field. Additionally, the sediment flowing in the estuary stream can vary in size, shape, colour and type of matter, leading to potential measurement discrepancies. It is important to note that this is not an issue unique to the sensor and calibration methodology presented in this work, but a general challenge for instruments designed to assess suspended sediment concentration. Although turbidity calibrations with formazine aim to standardize these instruments, they make little sense to use when the primary objective is to measure sediment transport.

The water velocity output was calibrated using a water circuit in the

laboratory with water pumps. The different flow rates produced by the pump intensity levels were measured to match the fluid velocity recorded by the sensor. Despite the efforts to conduct an effective calibration, the system used is somewhat rudimentary, lacks ground truth validation, and does not account for the disruption caused by the instrument to the natural flow. Thus, the measurements of water velocity are also subject to error when the calibration results are applied in different fluidic channels.

4.2. Cross-section and stream velocity profile dependencies

The errors associated with the calibrations are important for achieving precise measurements. However, the primary source of errors related to the field results pertains to the estimation methodology employed, particularly concerning water discharge. Equation (3) was used to estimate water discharge, which is a function of water velocity (directly measured by the sensor) and the cross-section of the estuary. As the results demonstrated, the sensor's installation location is subject to tidal changes, rendering the cross-section highly dynamic. For this study, we opted to follow a simplistic approach, defining a rectangular section area characterized by variable depth over time and constant width across the cross-section. However, in reality, the estuary's depth is not uniform along the cross-section and the stream width varies with the tide.

The water velocity measured by the sensor (at a single point along the cross-section) was also assumed to be constant throughout the cross-section. In water streams, the fluid velocity varies across depth, typically decreasing from the surface to the bottom. Near the surface, the velocity is higher due to reduced friction, while at the riverbed, frictional resistance decreases velocity significantly. Velocity profiles often exhibit a logarithmic or parabolic shape, with the highest velocity beneath the surface and the lowest near the bottom. The horizontal velocity profile, across the width of the stream, also varies, with the highest velocity typically found at the centre and decreasing towards the banks due to frictional resistance. Additionally, the mixing of fresh and salty water-fronts during high tides should also be considered. In estuaries with strong stratification, a salt wedge can form, creating a distinct interface between freshwater and seawater. This stratified flow leads to layered velocity profiles, where the upper layer (freshwater) moves differently from the lower layer (saltwater). Stratified conditions can induce shearing at the interface, increasing turbulence and complicating velocity profiles. All these factors combined can contribute to discrepancies in the estimations presented in this study.

4.3. Enhancing hydrodynamic estimations

The placement of the sensor within the water column significantly impacts the recorded measurements. Sensors positioned at different depth will register distinct velocity due to the vertical velocity gradient. Understanding the relationship between water velocity and depth in a river stream is crucial for precise hydrodynamic measurements and interpretations. Similarly, the sensor's location along the stream width also affects the recorded data. Calibration of the sensor may incorporate depth-dependent velocity profiles to ensure accuracy when applied in the field. Field studies should consider the sensor's intended position within the water column to accurately interpret data and estimate overall flow and suspended transport rates. However, this approach assumes measurement under smooth laminar flow conditions, which may significantly differ from the reality of estuarine streams.

Another potential solution involves increasing data collection points by deploying multiple sensors along the stream width and depth to refine the mesh and directly measure different velocity gradients. This solution underscores the importance of considering low-cost and energy-efficient designs during instrument development. The use of multiple sensors at different points of the cross-section provides direct measurements of the physical processes in study. However, installing a sensor

mesh presents challenges not only from an engineering perspective but also due to potential direct impacts on navigation and associated socio-economic issues it may entail.

A third and final suggestion is to utilize data gathered from sensors in computational hydrodynamic models. These models need to consider the characteristics of the stream channel (acknowledging its dynamic morphology and potential changes over time), as well as velocity profile gradients, fluid properties, and other factors influencing hydraulic dynamics. The data from field instrumentation can be used both as input and validation to improve the accuracy of these models. However, creating a generalized model applicable to all watersheds remains unfeasible. Each model should be tailored to the specific features of the area under study. Nevertheless, the integration of computational resources with field sensor data offers an appealing methodology not only for measurement and dynamics understanding but also for prediction and forecasting.

4.4. Biofouling in long-term monitoring

The field experiment was marked by an abnormal event of algae bloom, and the estuary stream was teeming with macro-fouling and other debris. On the fourth day of the experiment, the cantilever became entangled in algae, causing it to cease providing reliable measurements of water velocity. This issue is a common challenge for aquatic instrumentation, hindering long-term continuous monitoring without regular maintenance and sensor cleaning. For instance, traditional acoustic-based current meters are highly susceptible to algae attachment, which can obstruct the acoustic channels and disrupt measurements. An even greater concern is the formation of micro-biological growth on the surface of optical sensors (utilized here to measure suspended sediment concentration), which can introduce measurement drifts within just a few hours of instrument submersion. Biofouling poses a well-documented problem for sensors, prompting the emergence of various techniques in the literature to address this issue. We have also been focusing on this subject, mainly targeting optical instruments (Tiago Matos et al., 2023). The effectiveness of these techniques is crucial for empowering aquatic instrumentation in the years ahead.

5. Conclusion

This manuscript presents the development of a standalone sensor for *in situ* continuous estimation of sediment transport, addressing an existing gap in environmental monitoring. The instrument uses the measurements of water velocity, suspended sediment concentration, pressure (depth) and water temperature (for correction purposes) to estimate water discharge, total volume of water, sediment transport rate and total amount of sediment. The combination of multiple instruments to measure water velocity (current meters), turbidity and water level can be used to produce the same type of data. Nonetheless, a single device mainly focused on the estimation of sediment transport is a step forward in the study of a process with such importance in the dynamics of the watersheds.

The methodologies for the mechanical and electronic designs, assembling and fabrication are presented so the instrument can be replicated by others. During its development, the build of the sensor considered the material costs to allow massive replication (total of 70 € in raw materials) and energy efficiency to extend the operation time (250 mW taking measurements during 8 ms and 6 μW in sleep mode). The preparation for field experiments is also demonstrated. The device was calibrated in the laboratory to different flow velocity using a circuit with water pumps and to different suspended sediment concentration using samples of water with seashore sand. During these controlled experiments, the sensor presented a resolution from 0.001 g/L to 0.1 g/L in the 0–12 g/L range for the measurement of suspended sediment concentration and 0.05 resolution for 0–0.5 m/s range and 0.001 m/s resolution for 0.5–1 m/s range for the measurement of water velocity.

The instrument was validated in the estuary of Cávado River – Portugal to analyse its performance in real environment. The sensor was able to successfully measure the tidal cycles and consequent change of flow directions, and the suspended sediment concentration of the water course. These measurements allowed to estimate the water discharge and sediment transport rate during the different phases of tides, the daily total volume of water and the daily total amount of sediment passing through the estuary. The measurements provided by the sensor are in line with other estimations in the literature, however, it should be noted that the estimated results of water discharge and sediment transport are subject to error. The cross-section of the estuary was approximated to a rectangular shape, assuming uniform parameters for water depth, river width, water velocity, and sediment concentration throughout the area. However, this simplification does not accurately reflect reality. We provide considerations on the application of this type of instrumentation, including concerns about calibration methodologies, field installation designs, and insights on enhancing estimation accuracy.

During the field test, the sensor also suffered from biofouling. Both the transduction mechanisms to measure water velocity and suspended sediment stopped delivering reliable data after a couple of days. The biological attachment, and mainly the sludge encrustation, has been a problem during previous deployments of sensors in Cávado (Rocha et al., 2020, 2021, 2022). Biofouling is a problem that affects environmental sensors and has been preventing long-time continuous monitoring *in situ*. The scientific community has been paying attention to this problem and several technologies have been appearing in the literature. The effectiveness of these anti-biofouling techniques is a necessity to empower the instrumentation for aquatic environments.

Concluding, sediment transport plays an important role in coastal dynamics. However, there is still little information about this process, both because there is a lack of instrumentation for the effect and simulation and computational models lack accuracy. Information from sensors deployed *in situ* is needed to feed and validate said models. Since sediment transport is a complex combination of multiple parameters, it has been neglected for the purpose of *in situ* monitoring. We expect that the presented work provides the necessary methodologies to estimate this process and raise awareness for the potential of using this kind of device, or a combination of other available instruments, to understand sediment dynamics of coastal areas.

Funding

This work is co-financed by Fundo Europeu de Desenvolvimento Regional (FEDER) in project ATLÁNTIDA, NORTE-01-0145-FEDER-000040 and by national funds through FCT – Fundação para a Ciência e Tecnologia, I.P. under project SONDA (PTDC/EME-SIS/1960/2020).

CRediT authorship contribution statement

T. Matos: Writing – review & editing, Writing – original draft, Validation, Software, Methodology, Investigation, Formal analysis, Data curation, Conceptualization. **M.S. Martins:** Writing – review & editing, Validation, Supervision. **Renato Henriques:** Writing – review & editing, Validation, Supervision. **L.M. Goncalves:** Writing – review & editing, Validation, Supervision.

Declaration of competing interest

The authors declare that they have no known competing financial interests or personal relationships that could have appeared to influence the work reported in this paper.

Data availability

No data was used for the research described in the article.

Acknowledgements

The authors thank Câmara Municipal de Esposende and Museu Marítimo de Esposende for the support and conditions provided for the realization of the field tests. T. Matos thanks FCT for grant SFRH/BD/145070/2019.

Appendix A. Supplementary data

Supplementary data to this article can be found online at <https://doi.org/10.1016/j.jenvman.2024.121660>.

References

- Chalov, Sergey, Moreido, Vsevolod, Ivanov, Victor, Chalova, Aleksandra, 2022. "Assessing suspended sediment fluxes with acoustic Doppler current profilers. Case Study from Large Rivers in Russia." 6 (4), 504–526. <https://doi.org/10.1080/20964471.2022.2116834>, 10.1080/20964471.2022.2116834.
- Chien, Ning, Wan, Zhaohui, 1999. "Mechanics of Sediment Transport," June. <https://doi.org/10.1061/9780784404003>.
- Druiene, Flavie, Verney, Romaric, Deloffre, Julien, Lemoine, Jean Philippe, Chapalain, Marion, Landemaine, Valentin, Lafite, Robert, 2018. In situ high frequency long term measurements of suspended sediment concentration in turbid estuarine system (seine estuary, France): optical turbidity sensors response to suspended sediment characteristics. Mar. Geol. 400 (June), 24–37. <https://doi.org/10.1016/J.MARGEO.2018.03.003>.
- Duan, Jennifer G., Nanda, S.K., 2006. Two-dimensional depth-averaged model simulation of suspended sediment concentration distribution in a groyne field. J. Hydrol. 327 (3–4), 426–437. <https://doi.org/10.1016/J.JHYDROL.2005.11.055>.
- Furukawa, K., Wolanski, E., Mueller, H., 1997. Currents and sediment transport in mangrove forests. Estuar. Coast Shelf Sci. <https://doi.org/10.1006/ecss.1996.0120>.
- Guzman, C.D., Tilahun, S.A., Zegeye, A.D., Steenhuis, T.S., 2013. Suspended sediment concentration-discharge relationships in the (sub-) humid Ethiopian highlands. Hydrol. Earth Syst. Sci. <https://doi.org/10.5194/hess-17-1067-2013>.
- Kiat, Chang Chun, Ab Ghani, Aminuddin, Rozi, Abdullah, Zakaria, Nor Azazi, 2008. Sediment transport modeling for kulim river – a case study. Journal of Hydro-Environment Research 2 (1), 47–59. <https://doi.org/10.1016/J.JHER.2008.04.002>.
- Knighton, A. David, 1999. Downstream variation in stream power. Geomorphology. [https://doi.org/10.1016/S0169-555X\(99\)00015-X](https://doi.org/10.1016/S0169-555X(99)00015-X).
- Kostaschuk, Ray, Best, Jim, Villard, Paul, Peakall, Jeff, Franklin, Mark, 2005. Measuring flow velocity and sediment transport with an acoustic Doppler current profiler. Geomorphology 68 (1–2), 25–37. <https://doi.org/10.1016/J.GEOMORPH.2004.07.012>.
- Liu, Da, Alobaidi, Khaldoon, Valyrakis, Manousos, 2022. The assessment of an acoustic Doppler velocimetry profiler from a user's perspective. Acta Geophysica 70 (5), 2297–2310. <https://doi.org/10.1007/S11600-022-00896-3/FIGURES/7>.
- Lou, J., Ridd, P.V., 1997. Modelling of suspended sediment transport in coastal areas under waves and currents. Estuar. Coast Shelf Sci. 45 (1), 1–16. <https://doi.org/10.1006/ECSS.1996.0168>.
- Loureiro, Eduardo, Granja, Helena Maria, Pinho, José L.S., 2005. Morphodynamics of the Cávado estuary inlet (NW Portugal). <https://repositorium.sdum.uminho.pt/handle/1822/4637>.
- Matos, T., Faria, C.L., Martins, M.S., Henriques, Renato, Gomes, P.A., Goncalves, L.M., 2019. Development of a cost-effective optical sensor for continuous monitoring of turbidity and suspended particulate matter in marine environment. Sensors 19 (20), 4439. <https://doi.org/10.3390/s19204439>.
- Matos, T., Faria, C.L., Martins, M.S., Henriques, R., Gomes, P.A., Goncalves, L.M., 2020. Design of a multipoint cost-effective optical instrument for continuous in-situ monitoring of turbidity and sediment. Sensors 20 (11), 3194. <https://doi.org/10.3390/s20113194>.
- Matos, T., Rocha, J.L., Dinis, H., Faria, C.L., Martins, M.S., Henriques, Renato, Goncalves, L.M., 2022a. A low-cost, low-power and low-size multi-parameter station for real-time and online monitoring of the coastal area. Oceans Conference Record (IEEE) 2022-October. <https://doi.org/10.1109/OCEANS47191.2022.9977347>.
- Matos, T., Rocha, J.L., Faria, C.L., Martins, M.S., Henriques, Renato, Goncalves, L.M., 2022b. Development of an automated sensor for in-situ continuous monitoring of streambed sediment height of a waterway. Sci. Total Environ. 808 (February), 152164. <https://doi.org/10.1016/J.SCIOTENV.2021.152164>.
- Matos, Tiago, Faria, C.L., Martins, M., Henriques, R., Goncalves, L., 2019. Optical device for in situ monitoring of suspended particulate matter and organic/inorganic distinguish. In: OCEANS 2019 - Marseille, OCEANS Marseille 2019, 2019-June. Institute of Electrical and Electronics Engineers Inc. <https://doi.org/10.1109/OCEANSE.2019.8867080>.
- Matos, Tiago, Pinto, Vânia, Sousa, Paulo, Martins, Marcos, Fernández, Emilio, Henriques, Renato, Goncalves, Luis Miguel, 2023. Design and in situ validation of low-cost and easy to apply anti-biofouling techniques for oceanographic continuous monitoring with optical instruments. Sensors 23 (2), 605. <https://doi.org/10.3390/S23020605>. Page 605 23.
- Mitchell, S.B., Lawler, D.M., West, J.R., Couperthwaite, J.S., 2003. Use of continuous turbidity sensor in the prediction of fine sediment transport in the turbidity maximum of the trent estuary, UK. Estuar. Coast Shelf Sci. 58 (3), 645–652. [https://doi.org/10.1016/S0272-7714\(03\)00176-8](https://doi.org/10.1016/S0272-7714(03)00176-8).

- Manik Henry, Munandar, Firdaus, Randi, 2021. Quantifying suspended sediment using acoustic Doppler current profiler in tidung island seawaters. *Pertanika J. Sci. & Technol* 29 (1), 363–385. <https://doi.org/10.47836/pjst.29.1.21>.
- Nord, Guillaume, Gallart, Francesc, Nicolas, Gratiot, Soler, Montserrat, Reid, Ian, Vachtman, Dina, Latron, Jérôme, Pedro Martín-Vide, Juan, Laronne, Jonathan B., 2014. Applicability of acoustic Doppler devices for flow velocity measurements and discharge estimation in flows with sediment transport. *J. Hydrol.* 509 (February), 504–518. <https://doi.org/10.1016/J.JHYDROL.2013.11.020>.
- Papanicolaou, Athanasios, Thanos, N., Mohamed, Elhakeem, George, Krallis, Prakash, Shwet, Edinger, John, 2008. Sediment transport modeling review—current and future developments. *J. Hydraul. Eng.* 134 (1), 1–14. [https://doi.org/10.1061/\(ASCE\)0733-9429\(2008\)134:1\(1\)/ASSET/36E9167D-03E8-40BF-A4C9-304F21B4BD37/ASSETS/\(ASCE\)0733-9429\(2008\)134:1\(1\).FP.PNG](https://doi.org/10.1061/(ASCE)0733-9429(2008)134:1(1)/ASSET/36E9167D-03E8-40BF-A4C9-304F21B4BD37/ASSETS/(ASCE)0733-9429(2008)134:1(1).FP.PNG).
- Rocha, J.L., Matos, T., Martins, M.S., Lopes, S.F., Gomes, P.A., Henriques, R., Goncalves, L.M., 2021. Cost effective CTD for long term deployments in water columns. *Oceans Conference Record (IEEE)* 2021-September. <https://doi.org/10.23919/OCEANS44145.2021.9705844>.
- Rymszewicz, A., O'Sullivan, J.J., Bruen, M., Turner, J.N., Lawler, D.M., Conroy, E., Kelly-Quinn, M., 2017. Measurement differences between turbidity instruments, and their implications for suspended sediment concentration and load calculations: a sensor inter-comparison study. *J. Environ. Manag.* 199 (September), 99–108. <https://doi.org/10.1016/J.JENVMAN.2017.05.017>.
- Sahin, Cihan, Ozturk, Mehmet, Aydogan, Burak, 2020. Acoustic Doppler velocimeter backscatter for suspended sediment measurements: effects of sediment size and attenuation. *Appl. Ocean Res.* 94 (January), 101975 <https://doi.org/10.1016/J.APOR.2019.101975>.
- Schmeeckle, Mark W., 2014. Numerical simulation of turbulence and sediment transport of medium sand. *J. Geophys. Res.: Earth Surf.* 119 (6), 1240–1262. <https://doi.org/10.1002/2013JF002911>.
- Skarbøvik, Eva, Madsen van't Veen, Sofie Gyritia, Lannergård, Emma E., Wennig, Hannah, Stutter, Marc, Bieroza, Magdalena, Atcheson, Kevin, et al., 2023. Comparing in situ turbidity sensor measurements as a proxy for suspended sediments in north-western European streams. *Catena* 225, 107006. <https://doi.org/10.1016/J.CATENA.2023.107006>. May.
- Southard, John, 2006. "Threshold of Movement." *Special Topics: an Introduction to Fluid Motions, Sediment Transport, and Current-Generated Sedimentary Structures*.
- Wullenweber, Nellie, Hole, Lars R., Ghaffari, Peygham, Graves, Inger, Tholo, Harald, Camus, Lionel, 2022. SailBuoy ocean currents: low-cost upper-layer ocean current measurements. *Sensors* 22 (15), 5553. <https://doi.org/10.3390/S22155553>, 2022.
- Yanto, Dimiyati, Muhammad, 2023. Development, implementation and validation of sediment transport and erosion prediction (STEP) model. *Environ. Model. Software* 164 (June), 105686. <https://doi.org/10.1016/J.ENVSOF.2023.105686>.
- Zheng, Peng, Gumbira, Gugum, Li, Ming, van der Zanden, Joep, van der A, Dominic, van der Werf, Jebbe, Chen, Xueen, Tang, Xiaonan, 2023. Development, calibration and validation of a phase-averaged model for cross-shore sediment transport and morphodynamics on a barred beach. *Contin. Shelf Res.* 258 (April), 104989 <https://doi.org/10.1016/J.CSR.2023.104989>.